Available online at www.sciencedirect.com
SCIENCE DIRECT®
International Journal of Heat and Mass Transfer 48 (2005) 5417–5430
International Journal of HEAT and MASS TRANSFER
www.elsevier.com/locate/ijhmt

Study and modeling of heat transfer during the solidification of semi-crystalline polymers

R. Le Goff [a], G. Poutot [a], D. Delaunay [a,*], R. Fulchiron [b], E. Koscher [b]

[a] *Laboratoire de Thermocinétique de l'école polytechnique de l'université de Nantes, UMR CNRS 6607, rue Christian Pauc, BP 50609 44306 Nantes cedex 3, France*
[b] *Laboratoire des Matériaux Polymères et des Biomatériaux, IMP/UMR CNRS 5627, Université Claude Bernard, Lyon 1, 69622 Villeurbanne Cedex, France*

Received 16 December 2004; received in revised form 1 April 2005
Available online 12 September 2005

Abstract

Semi-crystalline polymers are materials whose behavior during their cooling is difficult to model because of the strong coupling between the crystallization, heat transfer, pressure and shear. Thanks to two original apparatus we study solidification of such a polymer without shear. Firstly the comparison between experimental results and a numerical model will permit to validate crystallization kinetic for cooling rate reachable by DSC. The second experiment makes it possible to analyze solidification for high cooling rate, corresponding to some manufacturing processes. It appears that crystallization has an influence on the thermal contact resistance.

Keywords: Semi-crystalline polymers; Crystallization; Thermal contact resistance

1. Introduction

Polymers are extensively used material so that the control of manufacturing techniques needs an accurate knowledge of heat transfer all along the processes. During the manufacturing, the cooling phase including solidification is often the most significant part of a cycle especially in the case of injection molding. In this phase, heat transfers are mainly by conduction in the polymer and this phenomenon is deciding in the behavior of an injected part.

Polymer materials are either amorphous or semi-crystalline. Heat transfers in amorphous polymers are simple to model. Indeed thermal properties are slightly variable, even during the solidification. Differently, semi-crystalline polymers are made of a crystalline part, which may represent more than half of the mass. This crystalline phase solidification induces a latent heat of crystallization and a variation of the thermal properties of the material. Thus, accurate modeling of heat transfers in these materials implies the description of:

- The kinetic of the heat source release during solidification.
- The evolution of the thermal properties due to the crystallization.

* Corresponding author. Tel./fax: +33 2 02 40 68 31 41.
E-mail address: didier.delaunay@polytech.univ-nantes.fr (D. Delaunay).

0017-9310/$ - see front matter © 2005 Elsevier Ltd. All rights reserved.
doi:10.1016/j.ijheatmasstransfer.2005.06.015

Nomenclature

Bi	Biot number
C_p	specific heat (J/kg K)
ΔE	energy variation on a length
G_0	growth rate
ΔH	total enthalpy of transformation (J/kg)
K	kinetic function of T
K_g	constant
L	thickness (m)
N_0	potential nuclei number
P	pressure (Pa)
R	perfect gaze constant
t	time (s)
TCR	thermal contact resistance (m^2K/W)
T	temperature (K)
T_∞	temperature where no macromolecule movement is possible (K)
T_f	equilibrium melting temperature (K)
T_g	glass transition temperature (K)
U^*	activation energy (J)

Greek symbols

α	transformation rate
λ	thermal conductivity (W/m K)
φ	heat flux (W/m^2)
ρ	density (kg/m^3)

Main subscripts

a	amorphous
ms	metal surface
ps	polymer surface
ref	reference
sc	semi-crystalline
*	relative to reduced form

- The potential dependence of the boundary conditions to the crystallization (thermal contact resistance in the case of solidification on the metallic wall of a mold).

In this paper, we will present a general methodology and its experimental validation to describe the coupling between heat transfer and solidification of the semi-crystalline polymers, including these three points. In some manufacturing processes, for example injection molding, the crystallization occurs under high cooling rate. We will take into consideration this case, the crystallization being described for two generic situations: moderate cooling rate trough the walls of a mold cooled by a controlled circulating fluid and high cooling rate by sudden contact with a cold metallic surface.

We will comment successively the results of two experiments dedicated to these two situations.

2. Experimental study

2.1. The material and its thermal properties

To keep a broad applicability to the results of this work, the material used for this work is a semi-crystalline polymer well-representative of this class of materials. It is a polypropylene which is one of the most common, and has the advantage to be the subject of a lot of papers on its kinetic (see for example the review of Hieber [1]). Ourselves, we used this polymer in previous studies [2–5] and it was precisely characterized. We successively recall its thermal properties and propose models. This material is an isotactic polypropylene from Solvay S.A. of commercial name is HV252.

To study heat transfer during crystallization of a polymer, it is necessary to take into account the dependency of thermal properties as a function of the temperature but also of the crystallization. Indeed, Sridhar and Narth [6] show for example that taking accurate temperature dependent data is crucial when polymer shrinkage is studied. The adequate parameter for crystallization as shown by Fulchiron [3] is the relative mass crystallinity α defined in Eq. (1)

$$\alpha = \frac{X_C}{X_\infty} \tag{1}$$

where X_C is the crystallinity depending on time, temperature and pressure, X_∞ is the crystallinity at the end of solidification.

In our study, pressure is very close to the atmospheric one, so heat capacity and density are taken independent of that parameter and given by Eqs. (2) and (3)

$$C_p(\alpha, T) = \alpha C_{p_{sc}}(T) + (1-\alpha) C_{p_a}(T) \tag{2}$$

$$\rho(P, \alpha, T) = \alpha \rho_{sc}(T) + (1-\alpha)\rho_a(T) \tag{3}$$

To identify the specific heat C_p in each phase of the polymer, DSC was used. Heat capacity is represented by a linear relation versus the temperature in Eq. (4)

$$\begin{aligned} C_{p_a} &= 3.10T + 2124 \\ C_{p_{sc}} &= 10.68T + 1451 \end{aligned} \tag{4}$$

The density is the inverse of the specific volume which is deduced from PVT diagrams. A reference paper was published by Fulchiron et al. [3] that permits to plot

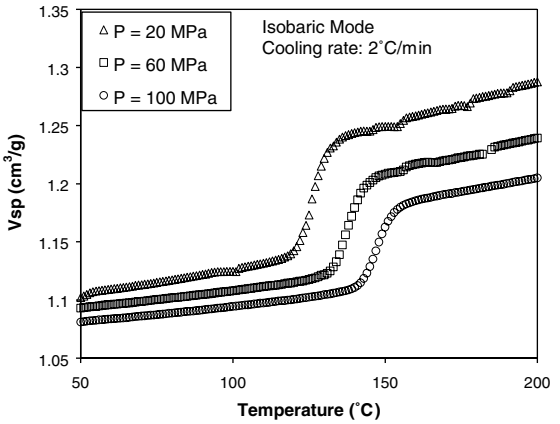

Fig. 1. PVT diagram of PP HV252.

these diagrams in Fig. 1. In our case, specific volume is obtained by Eq. (5)

$$V_a = 1.138 + 6.773 \times 10^{-4} T$$
$$V_{sc} = 1.077 + 4.225 \times 10^{-4} T \quad (5)$$

The thermal conductivity in the amorphous and semi-crystalline phase is also temperature dependant. A linear fitting gives Eqs. (6) and (7) for these conductivities (see previous papers already mentioned):

$$\lambda_a = -6.25 \times 10^{-5} T + 0.189 \quad (6)$$
$$\lambda_{sc} = -4.96 \times 10^{-4} T + 0.31 \quad (7)$$

With T in °C and λ in W/m K.

To model the effect of crystallization on the conductivity, several classical models are at our disposal. These well-known models have been carried out in the past by different authors for conduction trough heterogeneous media like composites but they can be relevant by substituting fiber ratio into relative crystallinity. Indeed the spherulites may be assimilated to spherical crystallites embedded in an amorphous matrix. We have compared the very classical one recalled in Eqs. (8)–(10) to the mixing rule.

- Maxwell's model [7]

$$\lambda = \lambda_a \frac{\lambda_{sc} + 2\lambda_a + 2\alpha(\lambda_{sc} - \lambda_a)}{\lambda_{sc} + 2\lambda_a - \alpha(\lambda_{sc} - \lambda_a)} \quad (8)$$

- Rayleigh's model [8]

$$\lambda = \lambda_a \left[1 - \frac{2\alpha}{\gamma + \alpha - \frac{C_1}{\gamma}\alpha^4 - \frac{C_2}{\gamma}\alpha^8} \right]$$
$$\text{with } \gamma = \frac{\lambda_a + \lambda_{sc}}{\lambda_a - \lambda_{sc}}, \quad C_1 = 0.3058, \quad C_2 = 0.034 \quad (9)$$

- Springer and Tsai's model [9]

$$\lambda = \lambda_a \left[1 - 2\sqrt{\frac{\alpha}{\pi}} + \frac{1}{B}\left(\pi - \frac{4}{\sqrt{1 - B^2\frac{\alpha}{\pi}}} \tan^{-1}\left(\frac{\sqrt{1 - B^2\frac{\alpha}{\pi}}}{1 + B\sqrt{\frac{\alpha}{\pi}}} \right) \right) \right]$$
$$\text{with } B = 2\left(\frac{\lambda_a}{\lambda_{sc}} - 1 \right) \quad (10)$$

In Fig. 2, the results corresponding to these models are reported. We note that the difference is negligible. This is due to the weak contrast between the conductivities in the amorphous and semi-crystalline phases. This result is well-known for composite materials and justifies the simplified model.

2.2. The crystallization kinetic

Crystallization is a mix between two occurrences: nucleation and growth. Nucleation involves the variation of two phenomena:

- A free energy variation ΔG_V associated to the transformation of liquid in solid. This term is negative for $T < T_f$.
- A free energy variation ΔG_S that is needed to form solid/liquid interfaces. This term is generally positive.

When plotted versus the size of a crystalline germ, $\Delta G_S + \Delta G_V$ presents a maximum. This corresponds to a potential barrier to be got over. In other words, the initial crystalline nucleus must be large enough to ensure that its growing will create a free enthalpy decrease. ΔG_S and ΔG_V depend on the degree of supercooling $(T_f - T)$. As a consequence, the number of germs N_0 that has been created as well as their rate of growth $G(T)$ increase when the degree of supercooling increases. Hence, the

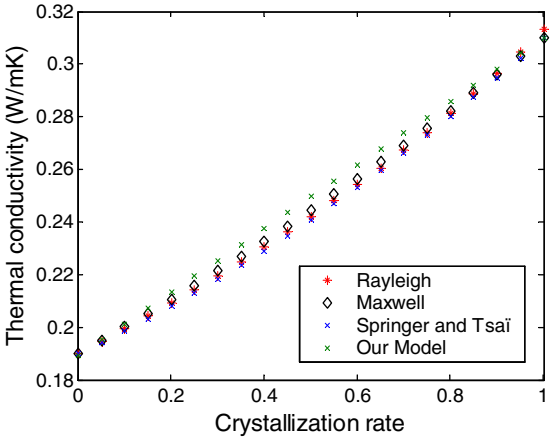

Fig. 2. Evolution of thermal conductivity versus relative crystallinity.

analysis of the crystallization in a range of low temperatures needs fast cooling experimental devices in order to reach this temperature range before the crystallization. However, the cooling rate of DSC is limited (typically 40 K/min) so it cannot be used for this purpose. For example, in the case of the present PP which crystallizes relatively rapidly, the DSC does not allow to obtain crystallization data for temperatures typically lower than 90 °C.

Avrami [10] had first developed a theory for crystallization in the case of isothermal crystallization. Ozawa [11] extended this theory to constant cooling rate. Finally Nakamura [12] completes it to crystallization whatever the cooling rate. Indeed, the Nakamura's theory gives a general expression Eq. (11) of the relative crystallinity as a function of the thermal history $T(t)$:

$$\alpha = 1 - \exp\left(-\left(\int_0^t K(T)\mathrm{d}u\right)^n\right) \tag{11}$$

A work due to Patel and Sprueill [13] allowed simplifying this complex relation into a more compact one, very useful for thermal modeling:

$$\frac{\partial\alpha}{\partial t} = n\cdot K(T)\cdot(1-\alpha)\cdot[-\ln(1-\alpha)]^{\frac{1}{n}-1} \tag{12}$$

To measure the temperature function $K(T)$, the polymer has been studied in a calorimeter DSC 7 from Perkin Elmer by Koscher [14]. The method consists in measuring the transformation rate from the heat flux balance in the sample, for which an example is shown in Fig. 3. The partial area method (the area under the crystallization peak at instant t over the total area) gives $\alpha(t)$. $K(T)$ is then directly deduced from Eq. (12).

For measurements, two cases are considered: isothermal crystallization ($K(T)$ is computed with Avrami's theory [10]) and constant cooling rate ($K(T)$ is computed with Ozawa's theory [11]).

The results obtained for $K(T)$ are regrouped in Fig. 4. As mentioned before, the DSC setting does not permit to have accurate measurements for cooling rates more than 40 K/min. That means that we cannot reach values

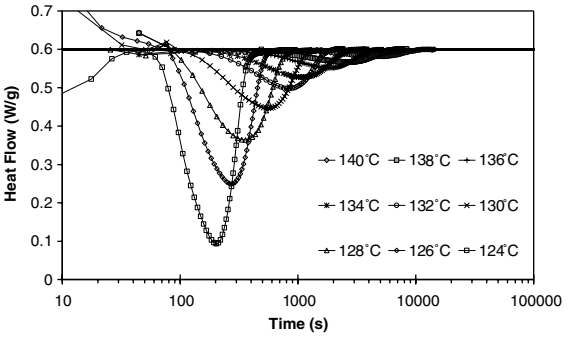

Fig. 3. Heat flows measured for isothermal crystallizations.

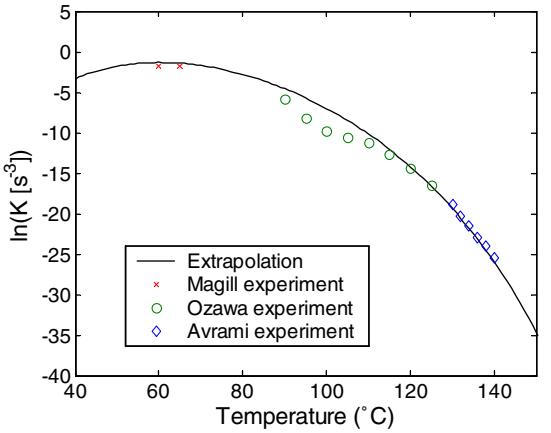

Fig. 4. Experimental value and model for function K.

of K for temperature under 90 °C. Magill [1] proposes values of K for 60 and 65 °C thanks to an optical method. We report these measurements on Fig. 4.

Then, this function has to be extrapolated in order to give an expression for the whole domain of temperature supposed to be reached during the injection process. If we suppose a perfect contact between the mold and the polymer, temperature can reach 40 °C. Perfect contact hypothesis is not reasonable however temperatures lower than 60 °C are not completely impossible to attain. Kosher [14] proposes an extrapolation based on the Hoffman–Lauritzen model according to Eq. (13). The author takes into account the number of active germs $N_0(T)$ and the growth rate $G(T)$ of polypropylene HV252

$$K(T) = \left[\frac{4}{3}\pi N_0(T)\right]^{\frac{1}{3}} G_0 \times \exp\left(-\frac{U^*}{R(T-T_\infty)}\right)\exp\left(-\frac{K_g}{T(T_f-T)}\right) \tag{13}$$

This equation is valid in the case of an instantaneous nucleation and for spherical entity growth. Koscher shows that isothermal crystallization occurs according to those two hypotheses. For PP HV252 of this study, $N_0(T) = \exp(1.56\times10^{-1}(T_f - T) + 1.51\times10^{1}))$, $G_0 = 2.83\times10^2$, $K_g = 5.5\times10^5$, $U^* = 6250$, $T_f = 210$ °C, $T_\infty = -30$ °C, $n = 3$. The curve corresponding to this relation is reported in Fig. 4.

2.3. Experiments at low cooling rate

The aim of this part is to validate the thermal model coupled with the crystallization kinetic model established by classical calorimetric methods on experimental results obtained in non-isothermal conditions (crystallization in the thickness of a piece). To have well-stated

boundary conditions and especially to avoid the effect of an unknown thermal contact resistance at the surface of the sample (see paragraph 4.1), we will apply a low cooling rate. In that perspective, we will use an experimental mold developed in the laboratory, called "on-line conductivimeter" [15]. This mold has first been built with the objective of measuring the thermal conductivity of polymers in their processing conditions. However the instrumentation of the mold is such that it can be applied to the characterization of the heat transfer during cooling provided thermal properties of the material are already known.

2.3.1. Principle of the on-line conductivimeter

The principle of the on-line conductivimeter is based on the injection of polymer around a metallic central plate. As shown in Fig. 5, material is sandwiched between the central plate and two symmetrical exchangers. Each of these exchangers is instrumented by a heat flux sensor and a thermocouple is implanted in the middle of the central plate. So the latter has a very significant advantage: it behaves like a thermocouple but it is impossible for it to move. Indeed temperature measurement is quite difficult especially with thermocouples placed in the polymer. Our experience [16] is that it is impossible to avoid their displacements during the crystallization, due to the induced internal stresses. During the solidification, they follow the local displacement lead by the shrinkage so they move. This was visually observed after cutting of samples. Therefore we dispose of an internal temperature measurement, the central plate being isothermal. Nevertheless this supposes to model the massive sensor constituted by the metallic plate.

The originality of the mold is to be heated before injection. This allows to cool the polymer after injection and to begin the solidification without shear, which is known to enhance crystallization. As shown in Fig. 6, it is constituted by two molding cavities separated by the removable central plate. This one is maintained by two insulating polymer rings resisting to high temperatures. These rings act as lateral walls of the molding cavity and permit to insulate the central plate in order to limit heat transfer in the radial direction. The central plate is equipped of a rubber-molded tail that permits

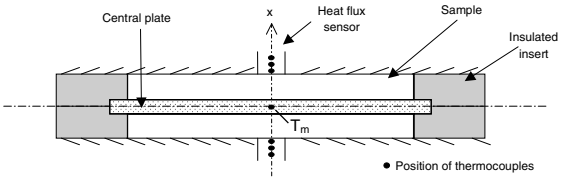

Fig. 5. Molding cavity of the conductivimeter.

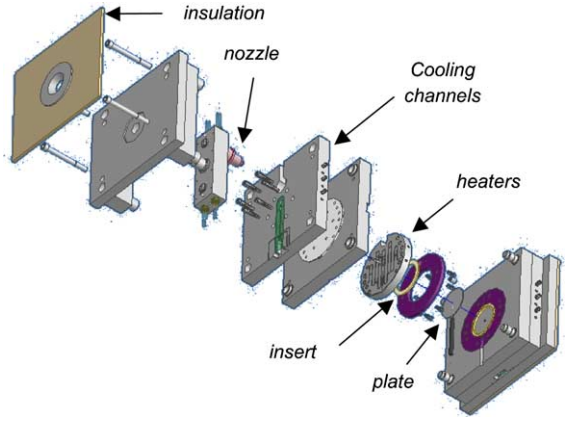

Fig. 6. Scheme of the whole mold [18].

to avoid the liquid polymer to flow outside the molding cavity, to keep the plate in a central position and to ensure the passage of thermocouple wires.

The mold is heated by electrical resistances. They are distributed in order to obtain an initial temperature as uniform as possible in the molding cavity before the arrival of the material. After injection, the cooling is achieved either by air or by water in an array of cooling channels. In addition, it was necessary to incorporate a system of hot channels which ensure the polymer to be maintained in a melted state in all the feeding circuit. Besides, the mold is equipped of a heated nozzle.

The characterization of heat transfer governing the polymer crystallization needs a specific instrumentation of the mold. The first goal of the conductivimeter being the measure of the thermal conductivity from the flux entering into the central plate, a type K thermocouple was placed in its center. A second thermocouple placed in the periphery of the central plate allows approaching the heat losses.

Moreover, two heat flux sensors have been symmetrically placed in the molding cavity. This kind of sensor permits to characterize heat transfer in a small thickness of wall close to the surface. In other words, quantity of heat which crosses the sensor, and lines of flows which result have to be identical with and without the presence of the sensor. Thus, this requirement imposes that the material and the surface quality of the mold and the sensor are the same.

2.3.2. Comments on Biot number relative to exchanges between the plate and the polymer

From the point of view of the cooling of the metallic plate, a Biot number may be defined as the ratio of internal resistance of the plate, $e/2\lambda$ and surface resistances that is to say the thermal contact resistance that exists between the metal and the polymer. The value of this number will give us information on the magnitude of

Table 1
Calculation of the Biot number

	Central plate
Thermal contact resistance (m^2 K/W)	5×10^{-4}
Thickness e (mm)	2
Thermal conductivity (W/m K)	36
Biot number	0.05

the thermal gradient in the plate during the injection cycle.

$$Bi = \frac{e}{2\lambda R} \tag{14}$$

The Biot number calculated in Table 1 for the central plate is very much lower than 1. We can suppose that the heat gradients are negligible at any time in the plate. In addition, thanks to the strongly capacitive character of the plate, this one reproduced the thermal phenomena of polymer in contact with it. Consequently, the thermocouple placed in the plate will give information on crystallization exactly as if it was placed in the heart of the polymer. In this sense, it constitutes an excellent thermal sensor, under the reserve that its inertia is large and must be taken into account in the analysis.

2.3.3. Experimental results

All the experimental results were obtained by using the following injection conditions: injection temperature: 220 °C, injection time: 5 s, holding pressure: 20 MPa.

Fig. 7 shows a characteristic evolution of the temperature measured by the different sensors during an injection cycle. We can estimate that the cooling rate reaches 17 K/min at the beginning of the cooling to decrease to 5 K/min at the end of the cooling. Furthermore, because of that slow cooling rate, the difference of temperature measured by the thermocouples of the heat flux sensor remains negligible. Then we will use the measure of the first thermocouple at the surface of the mold in the model, the heat flux being very difficult to estimate precisely with the heat flux sensor.

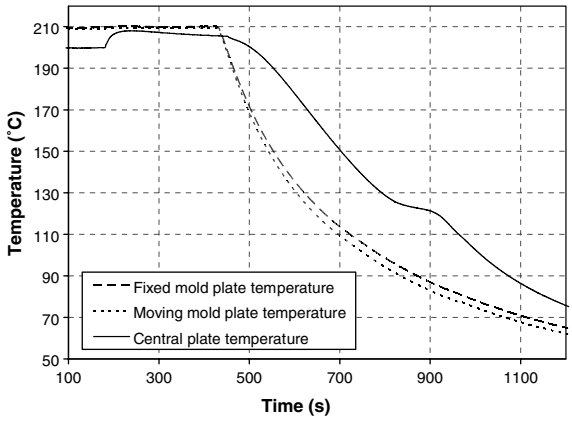

Fig. 7. Temperature evolution during cooling.

Before injection, the mold is almost isothermal but the central plate is slightly colder (a difference of 10 K between the central plate and the walls of the molding cavity). Approximately, at time $t = 180$ s, the temperature increases with the arrival of the hot polymer to slightly decreases afterwards. This phenomenon is due to a heat flux of losses, especially passing trough the "tail" of the central plate. This point is examined later. The polymer has conductivity ten times higher than the air, so the temperature difference between the plate and the molding cavity is much lower.

At time $t = 431$ s, the walls of the molding cavity are cooled trough the air cooling channels and their temperature quickly decreases. The temperature observed on the central plate exhibits an evolution characteristic of the cooling of a semi-crystalline polymer. It confirms the behavior which had been predicted by Le Bot [17]. Before the beginning of the solidification, the cooling is inside an amorphous material and the temperature decreases. At nearly 125 °C, a crystallization quasi-plateau appears. Then the cooling continues. The occurrence of a quasi-plateau is an important result which can give information on an "equivalent" crystallization temperature which can be used in the future for simplified models of the Stefan type or enthalpy method. The slope of the quasi-plateau, which is not perfectly horizontal as in the case of a material with a fixed solidification temperature, is to put in relation with the kinetics of crystallization.

It is significant to note the dissymmetry of cooling between the two walls of the molding cavities. Indeed the fixed mold is cooled less quickly. This difference of cooling is due to the internal design of the mold and of the cooling channels which are not symmetrical, and to the presence of the heating of the runners on the fixed part of the mold.

The mold was designed in order to have an initial temperature as homogeneous as possible in the molding cavity. However the evolution of temperatures at the beginning of injection reveals a difference between the plate and the walls in spite of the steady-state regime. To maintain in place the central plate, it is necessary to have a good mechanical holding. The polymer ring ensures this function. However, this is "paid" by heat losses on the lateral surfaces of the plate. Their evaluation is nevertheless important to compute with the temperature of the plate. The period before the cooling is used. It is a quasi-steady-state for which the temperature of the plate varies very slowly. The heat balance in the central plate can be written by Eq. (15):

$$\varphi_{\text{Polypropylene}} = -\frac{\mathrm{d}h}{\mathrm{d}t} + \varphi_{\text{Losses}} \tag{15}$$

$\varphi_{\text{Polypropylene}}$ is the heat flux passing across the polymer, which is simple to calculate. We consider here the polymer in a steady-state and a perfect contact between the mold and the polymer, the sum of thermal contact resistance on the boundaries of the molding cavity being an order of magnitude less than the polymer layer resistance. dh/dt is the enthalpy variation of the central plate for one m^2 of its surface. Considering that its temperature is uniform at T_m as explained in the previous paragraph, it is also simple to evaluate. As a consequence, the heat losses can be accurately evaluated before the cooling.

For all the experiments that we have done, a constant value was obtained, which gives a very good agreement between the computed temperature for the plate and its experimental evolution in the early time of the experiment, before the cooling (see for example on Fig. 12a for time less than 140 s). Several injections were carried out. In each of them at the beginning of the experiment, the losses exhibit different values. As a consequence, we will have to evaluate them before each simulation. Moreover, it is not unreasonable to suppose that the losses are function of time during the phase of cooling. Indeed, when the cooling is triggered, the temperature field in the environment of the molding cavity is modified. This perturbation, when it reaches the edges of the molding cavity, can modify heat losses. However, the measure is done in the center of the central plate so the perturbation is delayed before reaching the measurement area. Consequently, we can consider that the heat losses remain constant during a time period that it is necessary to evaluate. We consider that this period is inferior to 400 s. This choice is funded by the divergence between the measure and the modeling systematically observed for a longer time. Thus, to analyze the phenomenon during the crystallization and to limit the duration of this one so that crystallization occurs before 400 s, we will inject the polymer in a molding cavity regulated to a temperature close and just above the plateau observed in Fig. 7.

2.3.4. High cooling rate and zero shear device

The objective is to submit the melted polymer to boundary conditions with a cooling rate representative of some industrial processes, where a hot polymer is put into contact with a metallic surface (for example in injection molding). The polymer, under the shape of granules, is placed in a rubber-made ring with a low Young's modulus as shown in Fig. 8. The whole is located between two plates equipped with heating resistances (a fix lower plate P_2, and a removable upper plate P_1). The polymer is melted and is maintained to a constant temperature in order to reach a steady-state regime. Then, an air cooling system is triggered. A lateral movement is imposed to the superior heating plate P_1, and at the same time, the polymer is put into contact with a cold cylindrical plate P_0 moved down vertically.

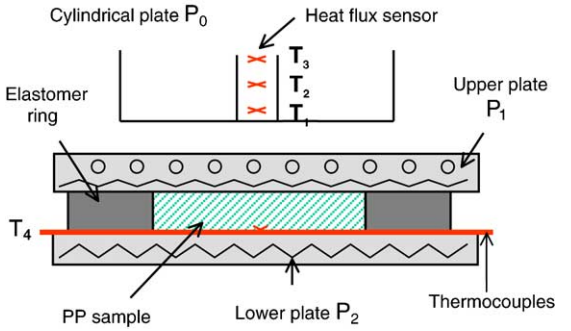

Fig. 8. Scheme of the rapid cooling device.

This cylindrical plate P_0, assimilated to the molding cavity wall, is equipped with a heat flux sensor in order to observe heat exchange between the hot polymer and the cold metallic plate. A thermocouple is placed between the polymer and the lower plate P_2. The thermo-electrical signal of the thermocouple is amplified and is recorded by an oscilloscope.

The non-intrusive heat flux sensor has been designed for previous studies by Quilliet [18], it is constituted of three thermocouples whose positions are known with precision. A classical sequential inverse method [19] is used to compute the mold surface temperature and the heat flux going through the polymer-mold interface from temperatures T_1, T_2 and T_3. The sensors were verified by using another heat flux sensor. This one is a very thin sensor manufactured by Captec. The inconvenient of this one is to be very sensitive to the pressure. The procedure consists in diving the plate P_0 on which the sensor was stuck by conductive grease in a bath of melting ice. The heat flux which goes across the Captec sensor enters in the surface of the plate P_0 and in our own sensor. Fig. 9 shows the very good agreement between the two measurements. The P_1 plate is equipped with a

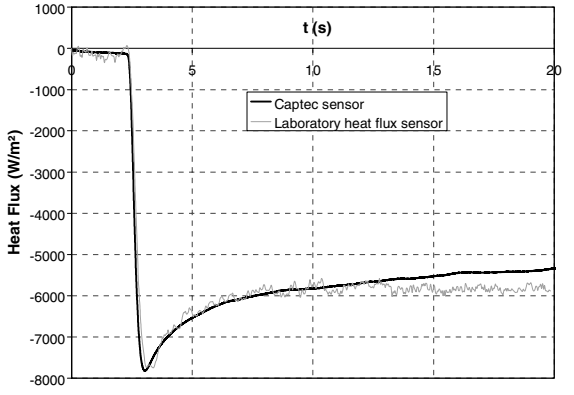

Fig. 9. Calibration of the heat flux sensor.

water cooling circuit on its surface that plays the role of a thermal screen, so that the sensor placed in the cylindrical plate P_0 is not sensitive to the heating, necessary to establish the polymer initial hot state. The temperature of the P_0 plate is controlled by a water circuit whose temperature is between 10 °C and 60 °C. The rubber ring maintains the sample when it is melted, follows the shrinkage thanks to its low enough module while permitting the tightness. For experiments on polypropylene, the material is melted at 190 °C and the cylindrical plate P_0 is maintained to 25 °C. The initial temperature is given by the thermocouple T_4 as we consider temperature is homogenous in the polymer before cooling.

The instrumentation of that apparatus makes it possible to compute the thermal contact resistance between the polymer and the metallic cold plate. It is defined by Eq. (16):

$$\mathrm{TCR} = \frac{T_{\mathrm{ps}}(t) - T_{\mathrm{ms}}(t)}{\varphi(t)} \tag{16}$$

In this equation, T_{ps} is the surface temperature of the polymer, T_{ms} is the surface temperature of the metal and $\varphi(t)$ is the heat flux going across the interface.

The surface temperature of the metal and the heat flux deduced from the heat flux sensor are computed for 40CMD8 steel in which the sensor and the cylindrical plate are made. For the three thermocouples T_1, T_2 and T_3 (cf. Fig. 8) we obtain curves as shown in Fig. 10. The time step for the acquisition is 5 ms. The surface temperature obtained with the classical Beck's algorithm is very close to the temperature T_1. The heating of the surface is very similar to the one observed on a mold [17], with an increase of approximately 10 K when the hot polymer comes into contact with the cold mold. Our experiment is well-representative of the injection molding situation, with negligible shear in the polymer.

Fig. 11 shows the heat flux evolution at the interface between the metal and the polymer. Heat flux is also obtained by Beck's algorithm. We have verified that the result is not sensitive to the number of future time steps. The very small data acquisition frequency is responsible of the good quality of this result. The heat flux evolution has a maximum. This is characteristic of a non-perfect contact. The value of the maximum is very consistent with the results of Le Bot [17]. In Fig. 11, we have reported the results of two different experiments, in the same conditions. We observe the excellent reproducibility, before 7 s. At this time an air bubble provokes the detachment of the polymer on the mold. The resistance increases, leading to the decrease of the heat flux. The bubble was visually observed to confirm this hypothesis. It is possible to go deeper in the analysis by computing the thermal contact resistance given by Eq. (16). For that we must know $T_{\mathrm{ps}}(t)$. The direct measure of this temperature is very difficult, without error due to the intrusive character of the sensors. Bendada et al. [20] for example uses infrared sensors with optic fibers. The conductivity of this one being very different of the conductivity of the mold, it may induce some error. In addition, if the polymer is not filled with black pigments, it is semi-transparent and the temperature is averaged on a thickness which may be not negligible [21]. The authors ensured that the polymer is opaque for the spectral bandwidth of the pyrometer. However, in the absence of alternative technique, this one may constitutes a good reference for comparison. In our study, $T_{\mathrm{ps}}(t)$ is obtained indirectly by computation. This one consists in using $\varphi(t)$ as boundary condition of the resolution of a direct problem of conduction in the polymer. We then obtain the temperature in any location of the polymer, especially on its surface. The modeling is presented in the next section.

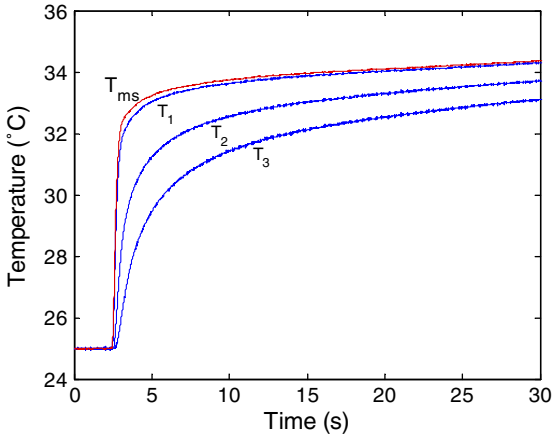

Fig. 10. Surface temperature of the metal.

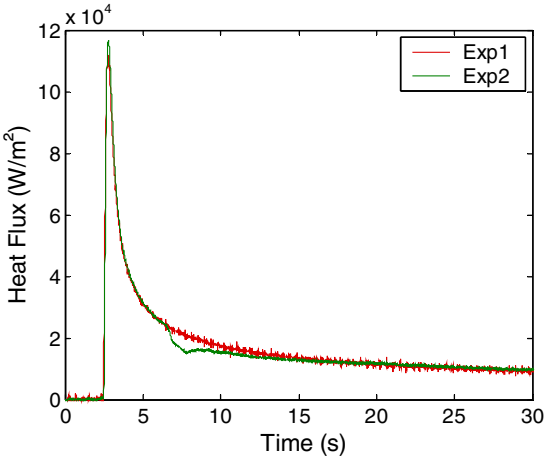

Fig. 11. Evolution of the heat flux.

3. Modeling of the experiments

The system to solve in order to describe heat transfer in the 1D configuration of the polymer parts of the two apparatus is constituted of Eqs. (17) and (18).

The kinetics is expressed by using the differential form of Nakamura's equation [12], Eq. (18). $K(T)$ is given by Eq. (13). The thermal properties are specified in the Section 2

$$\rho(P,\alpha,T)\cdot C_p(\alpha,T)\cdot\frac{\partial T}{\partial t}=\frac{\partial}{\partial x}\left(\lambda(\alpha,T)\cdot\frac{\partial T}{\partial x}\right)+\rho(P,\alpha,T)\cdot\Delta H\cdot\frac{\partial\alpha}{\partial t} \quad (17)$$

$$\frac{\partial\alpha}{\partial t}=n\cdot K(T)\cdot(1-\alpha)\cdot[-\ln(1-\alpha)]^{\frac{1}{n}-1} \quad (18)$$

This system has been solved by standard finite differences. In the case of the modeling of the on-line conductivimeter mold, the interface between the polymer and the metallic central plate is simulated by a thermal contact resistance. In a first approach, its value is chosen according to literature [20,22] at a value of $5\times10^{-4}\,m^2\,K/W$. We will study its influence further.

In the case of the rapid cooling apparatus, the boundary conditions are given by the thermocouple T_4 on one side (see Fig. 8) and by the heat flux sensor measurement on the other side. A difficulty is induced by the very fast heat source release at the interface, in the presence of a Neumann boundary condition. We have used an exact analytical solution of a similar problem to test the accuracy of our solution, detailed in Appendix A.

4. Validation of the model and discussion on the influence of crystallization on the boundary conditions

4.1. Conductivimeter mold

The objective of this section is to compare the computed temperatures in the metallic plate with the experimental one in order to see if heat transfer across the polymer and the coupling with crystallization are correctly modeled. The domain of temperature has been divided into three parts. For the first one, the polymer was injected to 220 °C in a mold maintained to the same temperature. Cooling was then triggered. The duration is limited to 400 s after the beginning of the cooling. The result is shown in Fig. 12a. Heat transfer occurs in the amorphous polymer. We observe that the agreement is very good, all along the experiment. The difference between computation and measure is less than 1 K.

Then, we have carried out an injection with a mold temperature of 150 °C, that is to say at a temperature for which the crystallization does not start during the setting of the initial quasi-steady-state. It will allow us to obtain crystallization before 400 s. The results are shown in Fig. 12b. The maximum temperature difference is 2.5 K at $t=930$ s. The agreement is very good, the plateau being very well-reproduced. That means a very good description of the source by the model and an

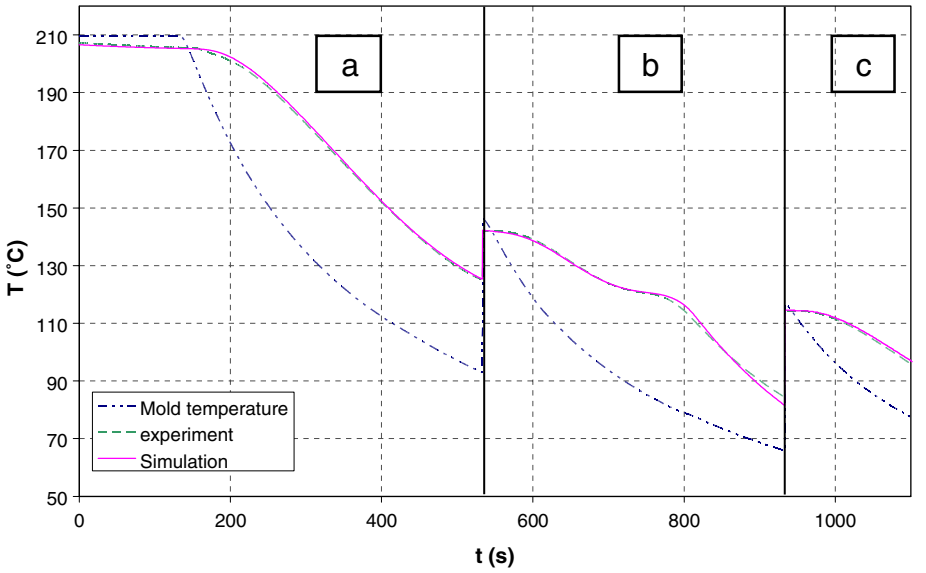

Fig. 12. Comparison between model and experiment.

accurate measurement and modeling of the thermal properties, in particular of their variation with the relative crystallinity.

After the complete solidification of the sample, a new heating under the melting temperature is done to obtain an initial state in solid. A cooling is then triggered. The results are shown in Fig. 12c. The differences are negligible, showing a very good characterization in solid phase.

We can conclude of this good agreement that heat transfer coupled with the crystallization are well-reproduced by the model. We show in Fig. 13, in the space temperature—relative crystallinity, the domain covered by the experiment. We notice that the crystallization takes place in the [109–125 °C] interval, for the entire sample. On Fig. 4, we can observe that this temperature range corresponds to a precise evaluation of the function $K(T)$. Indeed, in this temperature domain, DSC is very accurate. This explains the good quality of the comparison.

A question may be raised concerning the thermal contact resistances. In the preceding simulations, because we do not accurately know the value of this one, we took a value of 5×10^{-4} m^2 K/W. In order to check its influence on simulation, two calculations were done with a minimum value for the resistance of 10^{-5} m^2 K/W and with a maximum one of 10^{-3} m^2 K/W.

Fig. 14 presents the obtained results for these two simulations. To make the difference between the curves, a zoom is done in the crystallization area. Then we can observe a very low difference between the results, which

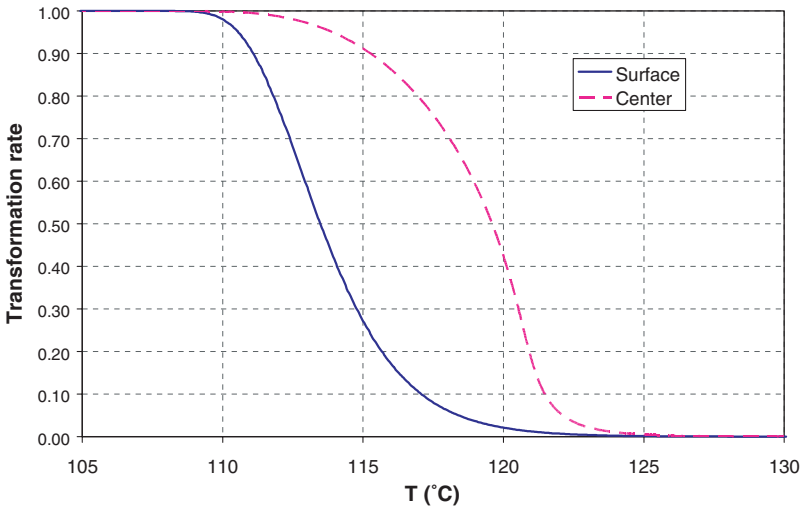

Fig. 13. Temperature domain of crystallization.

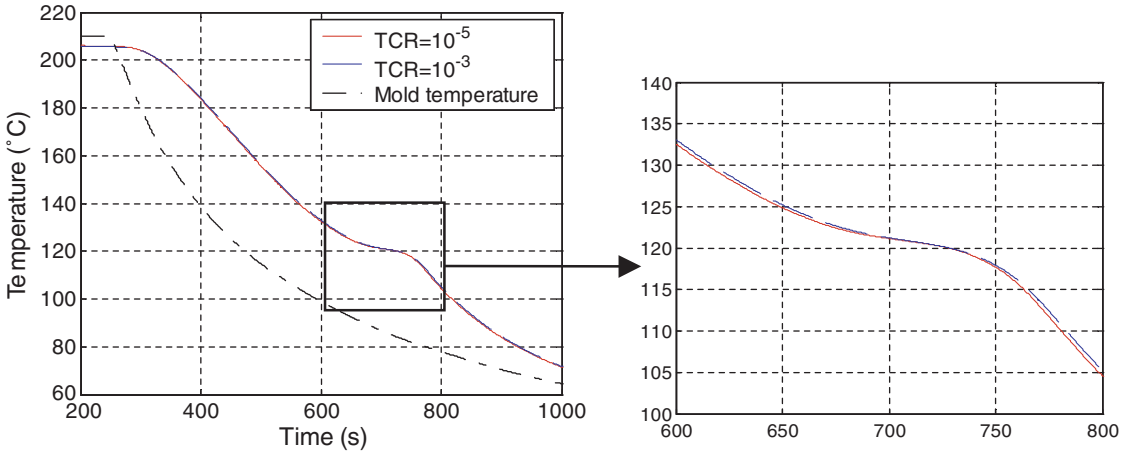

Fig. 14. Influence of thermal contact resistance.

indicates the negligible influence of the resistance. The model of coupling between heat transfer and crystallization is then validated.

4.2. Rapid cooling device

The objective of this section is to use the model which is now validated, to investigate the influence of the crystallization on the boundary condition to the interface between the polymer and the mold. Indeed, this one may be of influence in rapid cooling.

4.2.1. Temperature and crystallization at the polymer–metal interface

The thermal modeling permits to find the surface temperature of the polymer. So it is possible to observe the temperature evolution on each part of the polymer mold interface. Fig. 15 shows the behavior of the surface temperature of the polymer. After an abrupt decrease, this one reaches a minimum and we note that it corresponds to the beginning of the crystallization. Since crystallization is an exothermic phenomenon, it explains the small raise of the temperature during this one. For such high cooling rate, crystallization lasts approximately 3.5 s. When it is complete, the surface temperature of the polymer remains quasi-constant. This behavior is also observed at the beginning of the cooling in injection molding. We observe an important difference of temperature between the polymer surface and the mold. The temperature of the polymer during the crystallization remains 75 °C. We can see in Fig. 4 that this value is between the experiment of Magill and the highest cooling rate of DSC. We are in a temperature domain in which $K(T)$ has been measured and is known without extrapolation.

4.2.2. Thermal contact resistance

Thermal contact resistance is computed from Eq. (16). Its evolution is shown in Fig. 16. Just after the contact, its value is relatively high and it decreases to reach a minimum. The decrease is to put in relation with air which is trapped by the roughness of the surface. It takes some time to be evacuated. Then, the resistance becomes constant at 6.5×10^{-4} K m^2/W. This value is in good agreement with those found by Bendada et al. [20] or Yu [22], for higher pressure. It is also this value that has been found by Massé et al. [23] for amorphous polymer at low pressure, which is the case of this experiment before crystallization. The crystallization begins on the top of the roughness. Indeed, it is a location where heat flux density is maximum (cf. Fig. 17). The diameter d of the crystallized area increases. Two phenomena are in competition: the increase of the thermal conductivity of the solid polymer that decreases the thermal contact resistance and the increase of the air gap volume due to the shrinkage during the crystallization that increases the thermal contact resistance. This last phenomenon is preponderant, the air gap being the main cause of resistance. When the crystallization is complete, the thermal contact resistance continues to grow with a smaller rate. Between the sample and the metal, the air gap reaches the entire surface, no contact remaining between them. This is due to the small pressure that our apparatus

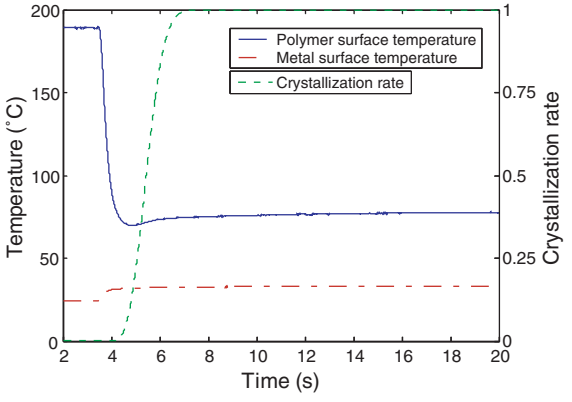

Fig. 15. Evolution of temperature on each side of the interface.

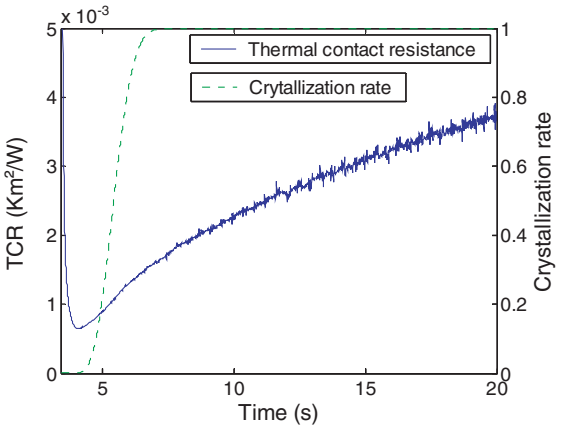

Fig. 16. Evolution of thermal contact resistance—influence of relative crystallinity.

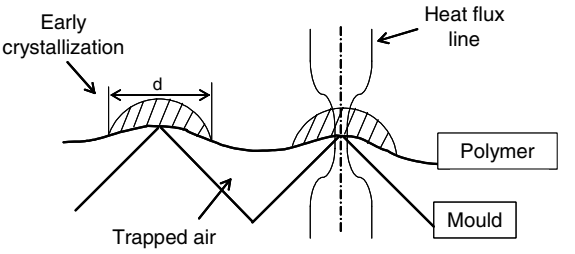

Fig. 17. Scheme of the metal–polymer interface at the beginning of the cooling.

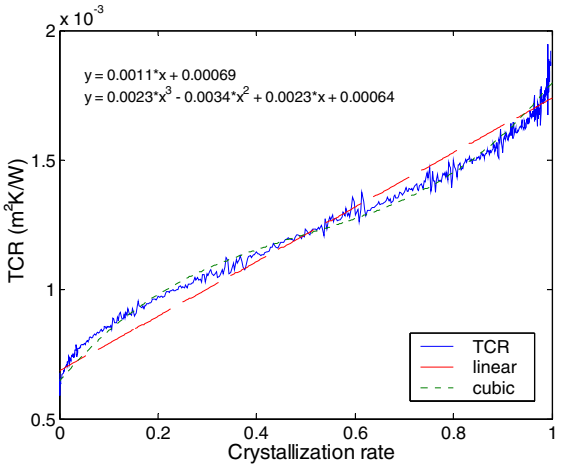

Fig. 18. Evolution of the thermal contact resistance versus relative crystallinity.

is able to maintain. It is not the case in injection molding where the effect of pressure has to be taken into account.

Fig. 18 shows the evolution of the thermal contact resistance versus the relative crystallinity at the surface. As we suppose, the influence of crystallization is not negligible on contact resistance. It is multiplied by 2 during the crystallization. The phenomenon which causes that increase is very complex and locally multi-dimensional. Its modeling needs a small scale analysis which will do the object of further work. Nevertheless it could be useful to have a relation between the crystallinity and the thermal contact resistance at the surface. We propose a linear relation: $\mathrm{TCR} = a_1 \cdot \alpha + a_2$ with a_1 and a_2 constants which values are indicated in Fig. 18. A cubic fitting is also proposed. The parameters are supposed to depend on the roughness which conditions the shape of the heat flux lines. Pressure is surely an important parameter but its influence has to be investigated. This model has to be improved for more generality.

5. Conclusion

Two apparatus were used to investigate coupling between heat transfer and crystallization of polymers whatever the cooling rate. They were designed so that no shear rate is applied on the polymer. The first one is constituted of a molding cavity in which a metallic plate is inserted. This metallic plate plays the role of an imbedded thermocouple which position is very well-known. A model was used to simulate heat transfer, in which the source of crystallization is represented by the Nakamura's equation. Moreover, thermal properties are taken dependant on temperature and relative crystallinity. We observe an excellent agreement between measured and computed temperature in the heart of the polymer part. It validates the crystallization model and the model used for the thermal property dependence. The observed behavior and these models are representative of a large class of semi-crystalline polymers.

The second apparatus allowed solidifying a polymer under high cooling rate. We underlined the effect of the thermal contact resistance which provokes an important temperature gap between the polymer and the metal surface. The use of the previously validated model permitted to show that this thermal contact resistance during the crystallization cannot be considered as constant. This result may be generalized to any semi-crystalline polymer. In our experiment, it was multiplied by two, with a quasi-linear evolution as a function of the crystallinity.

Acknowledgements

This work was partly supported by SCOOP Program with partners Moldflow, Legrand and Solvay. We wish to thank P. Kennedy, R. Zheng, H. Algave, J.M. Rossignol, M. Laplanche and V. Leo for their fruitful scientific discussions. This program was managed by G. Régnier that we especially thank. This work was also supported by Region Pays de Loire in the framework of pluri-annual grant. We express our gratitude to N. Lefevre for its crucial participation in the conception of the on-line conductivimeter and C. Le Bozec for his support during experiments.

Appendix A

We suppose a source which behavior is close to the crystallization one. It has a maximum, it starts of zero to reach zero at the end of the release. The total energy is equal to 92 kJ/kg, like for PP solidification. The duration of the source t_f is 6 s.

Heat equation and source may be written under a reduced form that is to say that all the parameters are written according to a reference value.

$$\frac{C_p^*}{Fo}\frac{\partial T^*}{\partial t^*} = \lambda^* \frac{\partial^2 T^*}{\partial x^{*2}} + \frac{1}{Fo \cdot Ste}[1 + \cos(t^* \cdot t_f + \pi)] \tag{19}$$

where Fo and Ste are respectively the Fourier's number and the Stefan's number whose equations are given by Eqs. (20) and (21)

$$Fo = \frac{\lambda_{\mathrm{ref}} \cdot t_f}{\rho C_{p_{\mathrm{ref}}} \cdot L^2} \tag{20}$$

and

$$Ste = \frac{\Delta H}{C_{p_{\mathrm{ref}}} \cdot T_{\mathrm{ref}}} \tag{21}$$

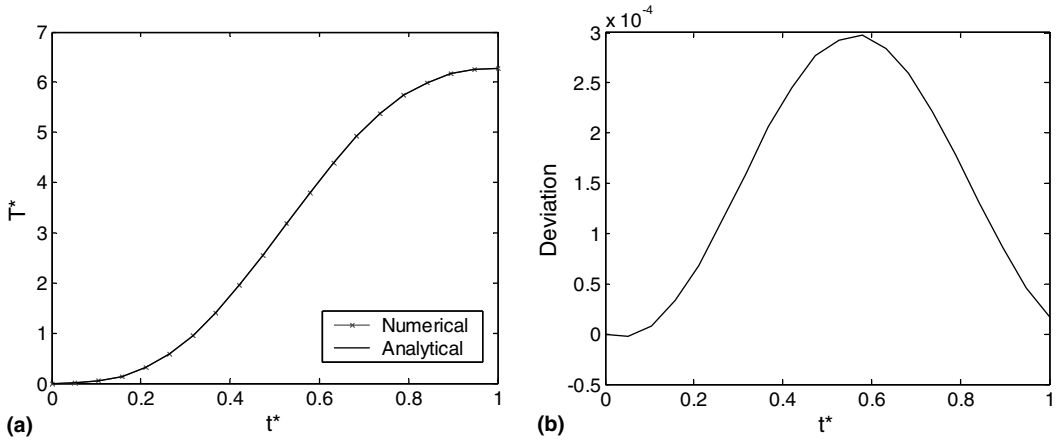

Fig. 19. Comparison and deviation between the numerical result and the exact solution for the surface temperature.

With the boundary conditions:

$$\lambda \frac{\partial T^*}{\partial x^*}(x^* = 0, t^*) = \lambda^* b \tag{22}$$

$$T^*(x^* = 1, t) = 0 \tag{23}$$

The solution is given by Eqs. (22) and (23)

$$T^*(x^*, t^*) = a x^{*2} + b x^* + c(t^*) \tag{24}$$

with a and b, two constants whose values are: $a = b = 3 \times 10^{-5}$. We have chosen: $L = 3$ mm, $t_f = 6$ s, $Ste = 1$, $Fo = 6.3 \times 10^{-2}$. $c(t)$ is given by

$$c(t^*) = \int [1 + \cos(t^* \cdot t_f + \pi) + 2aFo] \mathrm{d}t^* \tag{25}$$

Fig. 19a and b compare the numerical results with the exact solution. The time step is equal to 0.3 s and the number of nodes is 21. The difference is less than 3×10^{-4}, which remains small enough to validate our algorithm and to compute precisely the polymer surface temperature for imposed heat flux in the presence of the source.

References

[1] C.A. Hieber, Correlation for the quiescent crystallization kinetics of isotactic polypropylene and polyethylene terephtalate, Polymer 36 (7) (1995) 1455–1467.

[2] J.F. Luyé, G. Régnier, P. Le Bot, D. Delaunay, R. Fulchiron, PVT measurement methodology for semicrystalline polymers to simulate injection-molding process, J. Appl. Polym. Sci. 79 (2001) 302–311.

[3] R. Fulchiron, E. Koscher, G. Poutot, D. Delaunay, G. Régnier, Analysis of the pressure effect on the crystallization kinetics of polypropylene: dilatometric measurements and thermal gradient modelling, J. Macromol. Sci., Phys. 40 (3–4) (2001) 297–314.

[4] D. Delaunay, P. Le Bot, R. Fulchiron, J.F. Luye, G. Régnier, Nature of contact between polymer and mold in injection molding. Part I: Influence of a non-perfect thermal contact, Polym. Eng. Sci. 40 (7) (2000) 1682–1691.

[5] D. Delaunay, P. Le Bot, R. Fulchiron, J.F. Luyé, G. Régnier, Nature of contact between polymer and mold in injection molding. Part II: Influence of mold deflection on pressure history and shrinkage, Polym. Eng. Sci. 40 (7) (2000) 1692–1700.

[6] L. Sridhar, K.A. Narh, The effect of temperature dependant thermal properties on process parameter prediction in injection molding, Int. J. Heat Mass Transfer 27 (3) (2000) 325–332.

[7] J.C. Maxwell, A treatise on Electricity and Magnetism, Oxford University Press, 1904, pp. 361–372.

[8] L. Rayleigh, On the influence of obstacles arranged in rectangular order upon the properties of a medium, Philos. Mag. 34 (1882) 481–502.

[9] G.S. Springer, S.W. Tsaï, Thermal conductivities of unidirectional material, J. Compos. Mater. 1 (1967) 166–173.

[10] M. Avrami, Kinetics of phase change. I: general theory, J. Chem. Phys. 7 (1939) 1103–1112.

[11] T. Ozawa, Kinetics of non-isothermal crystallization, Polymer 12 (1971) 150–158.

[12] K. Nakamura, T. Watanabee, K. Katayama, T. Amano, Some aspect of nonisothermal crystallization of polymers. I. Relationship between crystallization temperature, crystallinity and cooling conditions, J. Appl. Polym. Sci. 16 (1972) 1077–1091.

[13] R.M. Patel, J.E. Sprueill, Crystallization kinetics during polymer processing analysis of available approaches for process modelling, Polym. Eng. Sci. 31 (1991) 730–738.

[14] E. Koscher, Effets du cisaillement sur la cristallisation du polypropylène: aspect cinétiques et morphologiques, Thèse de Doctorat, Université "Claude Bernard" Lyon 1, 2002.

[15] T. Jurkowski, D. Delaunay, Y. Jarny, R. Deterre, Mesure de la conductivité thermique des polymères dans les conditions d'injection, Réalisation d'un conductivimètre en ligne, Congrès Français de Thermique, Presqu'île de Gien, vol. 2, 2004, pp. 703–706.

[16] G. Poutot, Etude des transferts thermiques lors de la cristallisation d'un polymère semi-cristallin, Thèse de Doctorat, Université de Nantes, 2002.
[17] P. Le Bot, Comportement thermique des semi-cristallins injectés—Application à la prédiction des retraits, Thèse de Doctorat, Université de Nantes, 1998.
[18] S. Quillet, Transferts thermiques à l'interface polymère-métal dans le procédé d'injection des thermoplastiques, Thèse de Doctorat, Université de Nantes, 1998.
[19] J.V. Beck, B. Blackwell, C. St Clair, Inverse Heat Conduction III. Posed Problems, Wiley Interscience Publication, New York, 1985.
[20] A. Bendada, A. Derdouri, M. Lamontagne, Y. Simard, Analysis of thermal contact resistance between polymer and mold in injection molding, Appl. Thermal Eng. 24 (2004) 2029–2040.
[21] G.Y. Lai, J.X. Rietveld, Role of polymer transparency and temperature gradients in the quantitative measurement of process stream temperatures during injection molding via IRpyrometry, Polym. Eng. Sci. 36 (13) (1996) 1755–1768.
[22] J.C. Yu, J.E. Sunderland, C. Poli, Thermal contact resistance in injection molding, Polym. Eng. Sci. 30 (24) (1990) 1599–1606.
[23] H. Masse, E. Arquis, D. Delaunay, S. Quillet, P. Le Bot, Heat transfer with mechanically driven thermal contact resistance at polymer mold interface in injection molding of polymer, Int. J. Heat Mass Transfer 47 (2004) 2015–2027.